Molecular Crystals and Liquid Crystals Incorporating Nonlinear Optics

Publication details, including instructions for authors and subscription information:
http://www.tandfonline.com/loi/gmcl17

Band Structure Calculations for the Polaron Lattice in the Highly Doped Regime of Polyacetylene, Polythiophene, and Polyaniline

S. Stafström [a b] & J. L. Brédas [a c]

[a] Laboratoim de Chimie Theorique Appliquck, Centre de Recherches sur les Materiaux AvencBs, Facultes Universitaires Nobe-Deme de la Paix, B-5000, Namur, Belgium

[b] Department of Physics, Linköping University, S-581 83, Linköping, Sweden

[c] Maître de Recherches of the Belgian National Fund for Scientific Research, FNRS

Version of record first published: 28 Mar 2007.

To cite this article: S. Stafström & J. L. Brédas (1988): Band Structure Calculations for the Polaron Lattice in the Highly Doped Regime of Polyacetylene, Polythiophene, and Polyaniline, Molecular Crystals and Liquid Crystals Incorporating Nonlinear Optics, 160:1, 405-420

To link to this article: http://dx.doi.org/10.1080/15421408808083035

Mol. Cryst. Liq. Cryst., 1988, Vol. 160, pp. 405–420
Reprints available directly from the publisher
Photocopying permitted by license only

Printed in the United States of America

Band Structure Calculations for the Polaron Lattice in the Highly Doped Regime of Polyacetylene, Polythiophene, and Polyaniline

S. STAFSTRÖM† and J. L. BRÉDAS‡

Laboratoire de Chimie Théorique Appliquée, Centre de Recherches sur les Matériaux Avancés, Facultés Universitaires Notre-Dame de la Paix, B-5000 Namur (Belgium).

Band structure calculations are presented for the polaron lattice conformation in the highly doped regime of polyacetylene, polythiophene, and polyemeraldine. We have also performed calculations for the soliton lattice in polyacetylene and for the bipolaron lattice in polythiophene and polyemeraldine. The polaron lattice band structures are found to be in good agreement with the observed optical absorption and magnetic data for the three polymers which all exhibit a metallic-like behavior in their highly doped state. The polaron lattice band structures for polyacetylene and polythiophene are calculated to be very similar, which is consistent with the experimental trends. The polyemeraldine salt bipolaron and polaron band structures present a single defect band deep in the gap, instead of the two defect bands usually found in other conjugated systems. This peculiarity is related to the lack of electron-hole symmetry in polyaniline and leads to a modified picture for the electronic transitions appearing in the gap upon doping.

I. INTRODUCTION

Since the discovery a decade ago of high conductivity in doped polyacetylene, an enormous amount of work has been devoted to the understanding of the electronic properties of conducting organic polymers. In particular, much attention has focused on the precise nature of the metallic-like state which is reached at high doping levels.

In polyacetylene, a sharp increase in the Pauli susceptibility occurs at about 5% doping level, e.g. in sodium-doped polyacetylene.[1] Sim-

†Permanent address: Department of Physics, Linköping University, S-581 83 Linköping (Sweden).
‡Maître de Recherches of the Belgian National Fund for Scientific Research (FNRS).

ilar observations have also been reported for polythiophene, polyparaphenylene, and even for some polypyrrole samples.[2-4] Recently, the proton acid doping of polyemeraldine has attracted a great deal of interest.[5] In this case, Pauli susceptibility increases roughly linearly as a function of protonation level. This evolution has been explained on the basis of the formation of metallic islands.[5] Other properties of the metallic state such as optical conductivity in the far-IR region[6-8] and linear dependence of the thermopower[9-10] with temperature have also been shown to be present in these polymers.

In polyacetylene, a number of models have been suggested in order to rationalize the appearance of a metallic regime at high doping levels. Early on, it has been proposed that a simple closure of the Peierls gap was occurring, due to the removal of bond alternation.[11] More refined models have been worked out by Mele and Rice on the basis of a transition into a gapless incommensurate Peierls insulator.[12] Epstein has reported a summary of experimental data consistent with this approach[13] which seems more appropriate for disordered systems. More recently, Kivelson and Heeger[14] have pointed out that the sharp Pauli susceptibility increase at about 5% doping could be understood in terms of a first order phase transition from a soliton lattice to a polaron lattice. Photomodulation spectra of Ehrenfreund *et al.* on doped polyacetylene can be interpreted in this context.[15] It must be stressed, however, that calculations by Choi and Mele indicate that none of these models are currently able to address the persistence of the dopant-induced IR vibrational modes well into the metallic regime.[16] In polyemeraldine, the electronic properties of the fully protonated (salt) form have been shown to be consistent with the presence of a polaron lattice. The experimental magnetic and optical conductivity data[5] are in accord with the results of band structure calculations based on the polaron lattice conformation,[8] as will be discussed below. Despite the high current interest in polythiophene, related to the solubility and stability properties of its alkyl or vinylene derivatives,[17] the nature of the metallic regime in this compound has not been thoroughly investigated yet.

In this work, we present band structure calculations on highly doped polyacetylene, polythiophene, and polyemeraldine. Calculations are performed on different lattice conformations of the polymer chains. Polyacetylene is studied in the soliton and polaron lattice conformations, polythiophene and polyemeraldine in the bipolaron and polaron lattice conformations. The geometric structures of these polymers are sketched in Figure 1. Our calculations are aimed at investigating the electronic properties of different lattice conformations

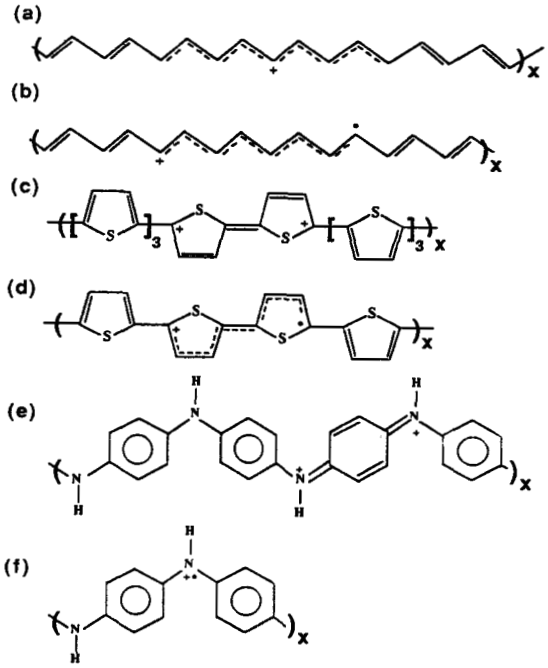

FIGURE 1 Sketch of the geometric structure of: (a) a positively charged soliton in trans-polyacetylene; (b) a hole polaron in trans-polyacetylene; (c) a hole bipolaron in polythiophene; (d) a hole polaron in polythiophene; (e) a hole bipolaron in polyemeraldine; (f) a hole polaron in polyemeraldine. These drawings also represent the unit cells taken into account for the band structure calculations performed in this work.

which are possible at high doping levels and relating them with the reported magnetic and optical data. Our general methodology is described in Section II. Results are presented and discussed in Section III. Conclusions of our work are stated in the last Section.

II. METHODOLOGY

A basic requirement in order to calculate the electronic properties of any molecule or solid is the knowledge of the geometry of the system. This turns out to be particularly important in conjugated systems where strong electron-phonon coupling is present. For example, it is by now well established that charge transfers between the polymer chains and a dopant or charge excitations introduce localized structural defects like solitons, bipolarons or polarons on

the chains.[18] Since only limited experimental information is available on the precise geometric structure of these defects, we have to optimize their geometry theoretically. The large spatial extension of these defects (~15 carbons or more) forces the geometry optimization problem to be treated by semiempirical techniques, rather than with *ab initio* methods. In this study, we rely on geometries obtained using the semiempirical Modified Neglect of Differential Overlap (MNDO) scheme.[19] Detailed descriptions of the calculation procedure are given elsewhere.[8,20,21] Only the main steps are outlined here.

Geometry optimizations in the presence of defects have been performed on the following oligomers: (i) $[H—(CH)_{40}—H]^{+\cdot}$ for the polaron and $[H—(CH)_{41}—H]^{+}$ for the soliton in trans-polyacetylene (our results are in full agreement with those reported previously by Boudreaux *et al.*[20]); (ii) $[H—(SC_4H_2)_6—H]^{+\cdot,2+}$ for the polaron and the bipolaron in polythiophene; and (iii) $[NH_2—(C_6H_4NH)_6—NH_2]^{+\cdot}$ for the polaron and $[NH_2—(C_6H_4NH)_7—NH_2]^{2+}$ for the bipolaron in polyemeraldine salt. The sizes of the oligomeric systems are chosen to be large enough as to avoid major influences of end effects in the optimized geometry of the defects. To reduce the number of variables in the optimization problem, we impose a central symmetric configuration in all oligomers; furthermore, all C—H bond lengths are held at a fixed value of 1.09 Å. Except for these restrictions, we allow for a full relaxation of the geometry of the system.

The band structure calculations are performed using the nonempirical pseudopotential Valence Effective Hamiltonian (VEH) method.[22,23] VEH band structure calculations have already been performed on a large number of conjugated polymers, including polyacetylene,[23] polythiophene,[24] and polyemeraldine.[8,25] The suitability of the VEH technique for describing the electronic structure of these compounds is illustrated by the excellent agreement between the photoemission (XPS or UPS) valence band spectra and the VEH-calculated spectra.[26] It is also our experience that the VEH band structures provide good estimates for the energies of the first optical transitions and are well suited for the studies of transitions involving the defect bands.

The geometries obtained from the MNDO optimizations on the (radical-)cation or dication oligomers are used to define the polymer unit cells in the band structure calculations. Each unit cell is chosen such as to contain a single defect. In this way, the number of monomers in the unit cell determines the doping level of the polymer chain. The unit cells and the corresponding doping levels (y) treated in this study are the following: (i) for trans-polyacetylene, the soliton

unit cell is chosen to be $(CH)_{17}^{+}$ ($y = 0.058$) and the polaron unit cell, $(CH)_{16}^{+\bullet}$ ($y = 0.0625$); (ii) for polythiophene, the bipolaron unit cell is $(C_4H_2S)_8^{2+}$ ($y = 0.25$) and the polaron unit cell, $(C_4H_2S)_4^{+\bullet}$ ($y = 0.25$); and (iii) for the polyemeraldine salt, the bipolaron unit cell corresponds to $(C_6H_4NH)_4^{2+}$ ($y = 0.50$) and the polaron unit cell to $(C_6H_4NH)_2^{+\bullet}$ ($y = 0.50$). We have used the common definition of the doping level, namely, y is equal to the charge per monomer. This way of denoting the doping level might sometimes be misleading; for example, in the polaron unit cells that we consider for trans-polyacetylene and polythiophene, there is exactly the same number of carbon atoms per unit charge, even though the doping levels as indicated by y are significantly different, $y = 0.0625$ and $y = 0.25$, respectively. Note that the unit cell of the soliton must contain an odd number of CH units while the bipolaron and the polaron unit cells both contain an even number of carbons and monomers.

Since the transition into the metallic state (as indicated for instance by a significant increase in Pauli susceptibility) is experimentally observed around $y = 0.05$ for trans-polyacetylene[1] and $y \sim 0.11$–0.14 for polythiophene,[2,4] the doping levels we have chosen lie into the metallic regime. As mentioned before, there exists no such sharp transition in the case of proton acid doping of polyemeraldine. The reason to choose $y = 0.50$ is based on the fact that this corresponds to the state of maximum conductivity and is consistent with the concept of segregation into fully protonated ($y = 0.50$) and unprotonated ($y = 0.0$) phases.[5]

III. RESULTS AND DISCUSSION

A) Polyacetylene

The VEH band structure of doped trans-$(CH)_x$ is presented in Figure 2a for the soliton lattice conformation ($y = 0.058$) and in Figure 2b for the polaron lattice conformation ($y = 0.0625$). Note that the reciprocal unit cell of the polaron lattice is about 6% larger than the one of the soliton lattice. The soliton band (band c in Figure 2a) is 0.74 eV wide and the subgaps appearing on both sides of this band are 0.62 eV and 0.60 eV for the lower and upper gaps, respectively. This indicates an almost perfect electron-hole symmetry close to the Fermi level. The polaron band structure shows two bands within the Peierls gap, bands b and c in Figure 2b. The widths of the lower and upper polaron bands are 0.95 eV and 0.94 eV, respectively. The two

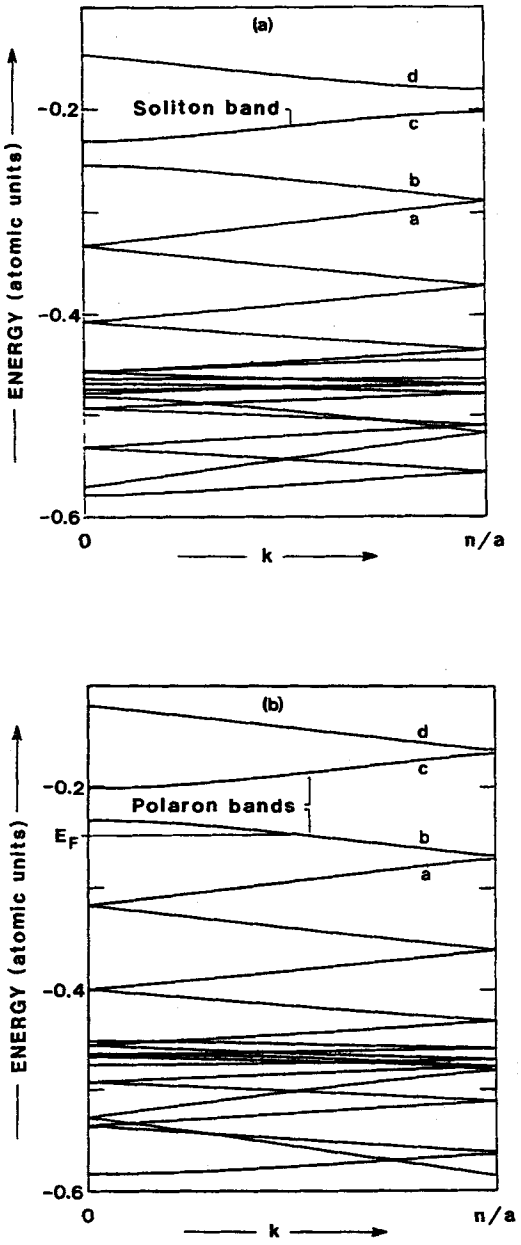

FIGURE 2 VEH band structures for trans-polyacetylene: (a) the soliton lattice at doping level $y = 0.058$ and (b) the polaron lattice at $y = 0.0625$.

polaron bands are separated (at $k = 0$) by 0.85 eV and are 0.09 eV away (at $k = \pi/a$) from the conduction or valence band edges.

A very interesting feature of our results is that the half-filled polaron band neatly fits into the gap (between the valence band and the soliton band) at the Fermi level of the soliton lattice. Therefore, excitations across this gap in the soliton lattice become comparable in energy to intraband excitations in the half-filled polaron band. This feature has important consequences for the comparison with experimental optical absorption data, as will be further discussed below.

The first interband transition in the soliton lattice (between bands *b* and *c* of Figure 2a) is calculated to onset at 0.6 eV and is followed by the $\pi-\pi^*$ transition between bands *b* and *d*. Taking the proper translational unit cell into account, we obtain a direct $\pi-\pi^*$ gap of 2.0 eV. Note that Jeyadev and Conwell have calculated that for the soliton lattice conformation, the oscillator strength of that $\pi-\pi^*$ transition is vanishingly small.[27] In the polaron lattice, we must take into account the intraband transition within the half-filled polaron band (band *b* in Figure 2b). Optical absorption within this band is expected in the far IR up to an energy roughly corresponding to the width of the polaron band, i.e. ~1.0 eV.

We may recall that optical transitions are strictly allowed only if *k*-vector (momentum) can be conserved. Kivelson and Heeger[11] argued, using an effective Hamiltonian for the polarons, that the polaron bands are essentially three-dimensional, a characteristic which provides many more degrees of freedom for the *k*-conservation rule to be fulfilled during intraband transition. Furthermore, we can expect some disorder effects to be present, which will destroy the symmetry of the lattice and thus the importance of the *k*-conservation rule.

Optical conductivity data on doped trans-polyacetylene (including the low frequency region)[6] show that above the critical doping concentration at which the polymer enters a metallic regime, there occurs a rounding of all optical transitions in the 0.5–2.5 eV region and a marked increase of absorption in the far IR. The first absorption peak shifts slightly down to 0.6 eV and the absorption previously related to the $\pi-\pi^*$ transition is no longer observed.

Clearly, above 5–6% doping, the soliton lattice conformation fails to explain the optical data in the far-IR region (since the excitation gap would be 0.6 eV in this case) as well as the magnetic data. Instead, the far-IR absorption can be well understood as originating from intraband absorption within the half-filled polaron band in the po-

laron lattice, as described above. The disappearance of the $\pi-\pi^*$ transition is in agreement with our calculations showing that in the polaron lattice the $\pi-\pi^*$ transition shifts to ~2.9 eV. Furthermore, for the polaron lattice, besides intraband excitations, optical transitions at 1.3 eV (from band *a* to band *b*), 1.6 eV (from band *b* to band *c*), and 2.8 eV (from band *b* to band *d*) are also predicted. This is in qualitative agreement with the rounding of the absorption data between 0.5 eV and 2.5 eV. Disorder effects can also lead to further rounding of these absorptions since around the doping levels where the metallic transition takes place, the widths of the polaron (or soliton) bands are very dependent on the actual doping levels. Indeed, the widths of the defect wavefunctions being of the order of 15–20 sites, slight local modifications in the actual doping level can significantly change the overlap between defect wavefunctions.

B) Polythiophene

The band structure of polythiophene in the bipolaron and polaron lattice conformations for $y = 0.25$ are shown in Figure 3a and 3b, respectively. Note that the length of the reciprocal unit cell in the bipolaron lattice is about half the one of the polaron lattice and contains twice as many bands. A comparison of the main features of the band structures for the two lattice conformations calls for the following remarks:

(i) Conceptually, if we go from the polaron lattice (Figure 3b) to the bipolaron lattice (Figure 3a), the two polaron bands (*b* and *c* in Figure 3b) are split into four bands (*b*, *b'*, *c*, and *c'* in Figure 3a), the middle two ones (bands *b'* and *c* of Figure 3a) residing in the gap as bipolaron bands; it is therefore apparent that the $\pi-\pi^*$ gap (between bands *b* and *c'*) in the bipolaron lattice is smaller than that (between bands *a* and *d*) in the polaron lattice.

(ii) The Fermi level appears at about the same energy in both cases.

(iii) The bipolaron bands lie deeper into the intrinsic bandgap.

The differences in the band structure between the two lattices suggest a description in which *the bipolaron lattice is the result of a dimerization of the polaron lattice*. The dimerization is driven by the lowering of the electronic energy of the system when an energy gap opens up at the Fermi level, i.e. a Peierls distortion. A schematic representation of the polaron and bipolaron band structures is given in Figure 4. This figure clearly illustrates the closure of the Peierls gap as the system is driven from a "dimerized" bipolaron lattice

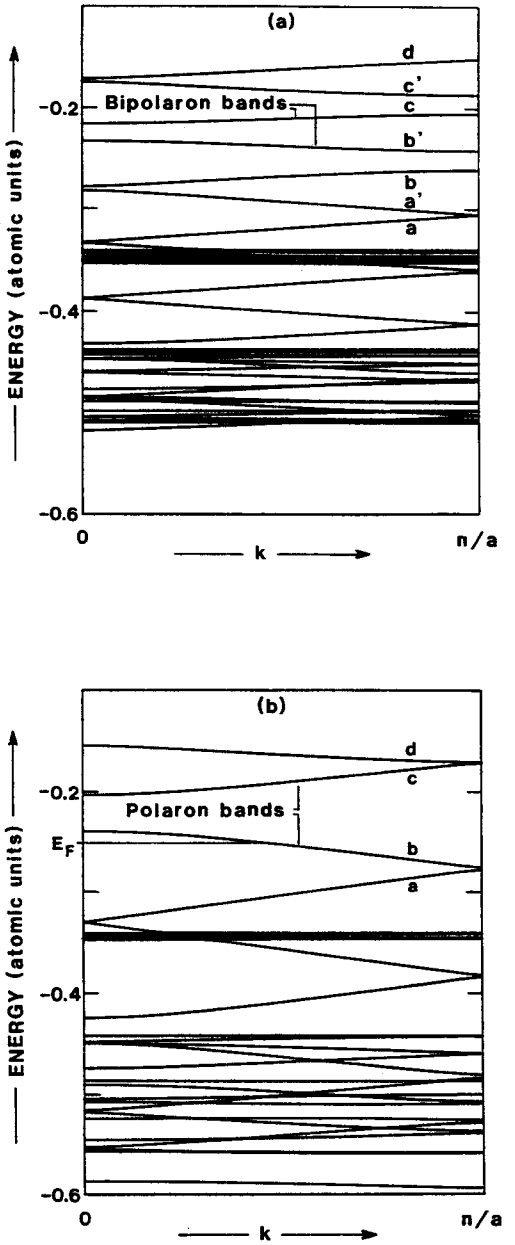

FIGURE 3 VEH band structures for polythiophene at doping level $y = 0.25$ for: (a) the bipolaron lattice and (b) the polaron lattice.

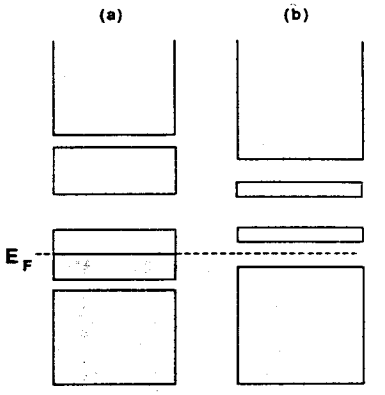

FIGURE 4 Schematic representation of the band structure at high doping level for: (a) the polaron lattice and (b) the bipolaron lattice, in a polymer such as polythiophene.

conformation (with an 8-monomer long unit cell) towards a polaron lattice conformation (with a 4-monomer long unit cell).

The widths of the lower and upper bipolaron bands are 0.28 eV (band b' in Figure 3a) and 0.26 eV (band c in Figure 3a), respectively, i.e. the electronic structure is symmetric around midgap. This feature also holds for the polaron bands, which are calculated to be 0.98 eV (band b in Figure 3b) and 0.85 eV (band c in Figure 3b) wide. We note that these values are almost identical to the widths of the polaron bands in trans-polyacetylene. Actually, by comparing the shape of the polaron bands in these two polymers (Figure 2b for trans-polyacetylene and Figure 3b for polythiophene), it is hard to notice any significant differences, the narrow subgaps between bands a and b, and bands c and d being also very similar. This similarity originates from the facts that: (i) there is almost no sulfur contribution to the lower polaron band in polythiophene; (ii) the carbon backbone in polythiophene resembles that of cis-polyacetylene; and (iii) the charge per carbon is formally the same (0.0625) in both cases.

The first interband transition in the bipolaron lattice, between bands b and b' Figure 3a, appears at 0.5 eV. It is evident from the comparison between the polaron and bipolaron lattice band structures presented in Figure 3 that this transition has its correspondence in an intraband absorption of the half-filled polaron band. Such an absorption onsets at zero energy and can extend up to about 1.0 eV, i.e. the polaron bandwidth.

For higher photon energies, we note that the bipolaron lattice would present a transition between bands b and c with an onset at 1.5 eV, followed by a transition between bands b and c' (the

$\pi - \pi^*$ transition) at 2.0 eV. These two transitions join into one in the polaron lattice (transition between bands *b* and *c*), which we predict to onset at 1.7 eV. Furthermore, for the polaron lattice there are also transitions between bands *a* and *b* which starts at 1.4 eV and between bands *a* and *c* which starts at 2.8 eV. Finally, we observe that the π–π^* transition in the polaron lattice has its correspondence in transitions between states deep into the valence and conduction bands of the bipolaron lattice, and consequently, appears at a much higher energy than in the bipolaron lattice. The transition is calculated to onset at 2.9 eV, which is similar to the value found for the polaron lattice conformation of trans-$(CH)_x$. No sharp transition is experimentally found in the 2–3 eV region,[7,28] in agreement with the polaron lattice model.

As a result of the similarities pointed out above between the polaron lattice band structures in trans-polyacetylene and polythiophene, it is expected that, if the polaron lattice model is correct, the experimental absorption spectra of trans-polyacetylene[6] and polythiophene[7] should be very similar. This is actually the case if we compare, for example, the data given in Refs. 6 and 28 and Ref. 29. At high doping, both polymers exhibit an absorption tail extending into the far-IR region and a rather symmetric peak at 0.6 eV (which can be understood in terms of an intraband transition within the half-filled polaron band) as well as very broad absorptions in the 1-3 eV region.

C) Polyemeraldine

The band structures for the bipolaron lattice and the polaron lattice in polyemeraldine salt are presented in Figures 5a and 5b, respectively. The unit cell of the bipolaron lattice is twice that of the polaron lattice, as in the case of polythiophene. We immediately observe that the almost perfect electron-hole symmetry present in trans-polyacetylene and polythiophene is not present in polyemeraldine. Only one polaron and one bipolaron band (bands *c* and *c'* in Figures 5a and 5b, respectively) appear deep in the gap, instead of the two deep defect bands found in all other conducting polymers studied so far. Note that the schematic representation of the bipolaron and polaron band structures given in Figure 4 *does not apply to polyemeraldine*. Actually, the conduction band in polyemeraldine is almost completely flat because, for symmetry reasons, there is no interaction between the π systems of the individual phenyl rings of the polymer chain for this band. As a result, the defect (polaron or bipolaron) band orig-

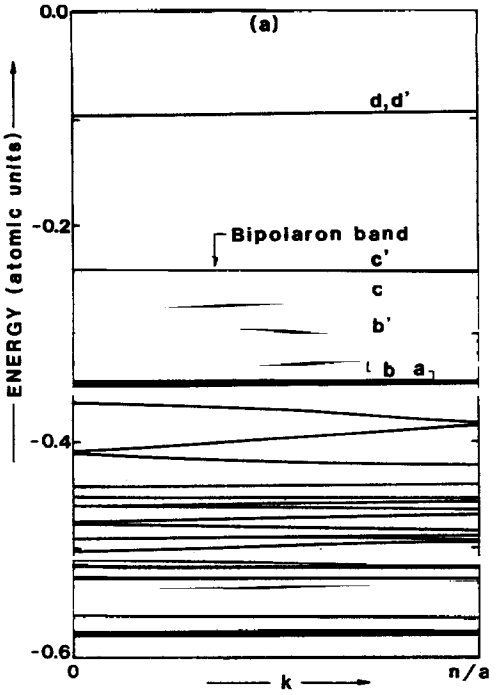

FIGURE 5 VEH band structures for polyemeraldine salt at doping level $y = 0.50$ for: (a) the bipolaron lattice and (b) the polaron lattice.

inating from the conduction band remains very shallow and is hardly distinguishable from it. This has interesting consequences since the first optical transitions, which usually involve both defect bands, are expected here to involve only the lower defect band.

Even though the doping level is high, we observe that the lower bipolaron band is narrow, its width being merely 0.1 eV. This is due to the fact that the bipolaron defect is mostly localized on a single quinoid-like ring. In the polaron conformation, the polaron bandwidth is larger, in our calculation 1.1 eV. The first interband transition in the bipolaron lattice occurs between bands c and c' and onsets at 0.6 eV. Transitions including higher unoccupied bands do not appear for energies below 3 eV. Instead, there would be low lying absorptions due to the promotion of electrons from deeper valence bands into the lower bipolaron band. In particular, a strong absorption to be due to the transition between the very flat band a and the likewise flat bipolaron band is expected at 2.7 eV. As we discussed for trans-polyacetylene and polythiophene, we expect the half-filled polaron

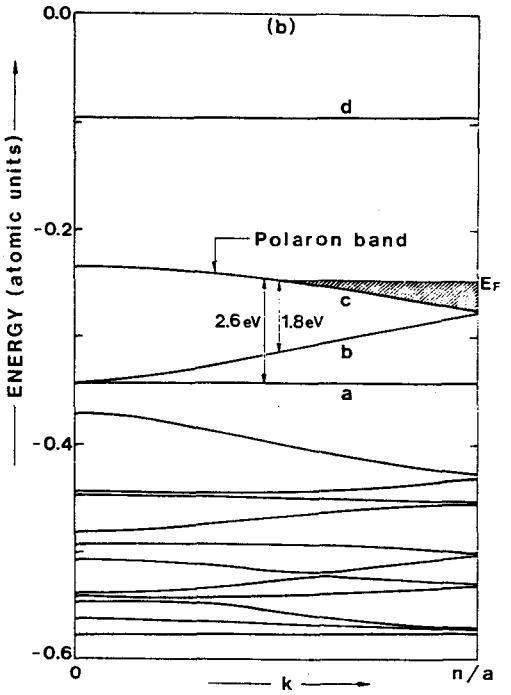

FIGURE 5 (*continued*)

band to allow for intraband transitions up to roughly 1.1 eV, the polaron bandwidth. This transition should be followed by interband transitions between bands *b* and *c* (1.8 eV), and bands *a* and *c* (2.6 eV).

The experimental absorption data for polyemeraldine salt show a broad asymmetric absorption peaked at 1.5 eV containing a long absorption tail extending into the far IR region.[8] The shape of this absorption is different from the low energy peaks in trans-polyacetylene and polythiophene. Our interpretation is that the long tail at the low energy side of the peak originates from the intraband absorption in the half-filled polaron band. This absorption is smoothly connected with the *b* to *c* interband transition, which we calculate to be at 1.8 eV. The width of the far IR absorption is experimentally determined to be ~1.0 eV, in very good agreement with our calculated width of 1.1 eV for the polaron band.[8] Contrary to what is observed in trans-polyacetylene and polythiophene, a second clear absorption is seen in polyemeraldine salt. This absorption peaks at 2.8 eV, i.e. in agreement with the *a* to *c* transition of the polaron

lattice. Further discussion of the agreement between our calculations and the experimental data can be found in Ref. 8.

IV. CONCLUSIONS

As noted in the Introduction, the sharpness of the transition into the metallic state for trans-polyacetylene and polythiophene is characteristic of a first order phase transition. It is then strking that, by following the evolution of the optical properties as a function of doping, no dramatic changes do occur when the critical concentration is reached. The low energy peak is almost unchanged and the $\pi-\pi^*$ transition exhibits a gradual decrease in oscillator strength with doping level. The major change is the appearance of far IR absorption which is observed in the highly doped state but not at low doping levels. It is therefore important that we have been able to show that these small changes agree very well with the picture of a transition into a polaronic metal.

At the crossover from the soliton lattice to the polaron lattice in trans-polyacetylene, the *interband* transition between the valence and the soliton bands is replaced by an *intraband* transition within the half-filled polaron band. Since the polaron band fits into the energy gap between the valence band and the soliton band, no major changes in the excitation properties are expected except for the onset of far-IR activity, in excellent qualitative agreement with the experimental findings. In polythiophene, the similarities between the situations before and after the possible crossover from a bipolaron lattice to a polaron lattice, are even more evident since the overall features of the band structure are the same for both lattice conformations (see Figures 3a and 3b). The main difference resides in the appearance of a finite density of states at the Fermi level when the bipolaron to polaron lattice transition takes place.

Our study of the different configurations of polyemeraldine must, however, be interpreted in a different way. It is expected that the polaron lattice is always present in the polymor as a result of phase segregation between metallic islands and undoped phases.[5] This peculiarity leads to a linear increase in Pauli susceptibility as a function of protonation. Thus, we do not intend to describe the evolution of the electronic properties of this polymer as we did for trans-polyacetylene and polythiophene, where we were arguing in terms of a transition from the band structure of Figures 2a or 3a to the band structures of Figures 2b or 3b, respectively. What we have demonstrated

is that, at a doping level $y = 0.50$, the polaronic metal model agrees much better with the experimental data than the bipolaron lattice model.

Finally, we would like to stress the following. Our band structure calculations can only provide a qualitative picture, since at this stage we are not in a position to follow the energetics of the crossover from a soliton/bipolaron lattice to a polaron lattice (which could be driven by three-dimensional and/or Coulomb effects). However, we believe that the polaronic metal description explains very well the optical and magnetic properties for high doping levels of the three polymers included in this study. Stimulated by this finding, it will be a challenge to find quantitative results, not only with regard to the optical properties, but also as concerns the stability of the different configurations and how disorder, Coulomb, and three-dimensional effects can influence the polymer properties in the highly doped state.

Acknowledgments

We are grateful to the Belgian National Fund for Scientific Research (FNRS), IBM-Belgium, and the Facultés Universitaires Notre-Dame de la Paix (FNDP) for the use of the Namur Computing Facility (SCF). One of us (S.S.) is supported by FNDP, the Swedish Natural Science Council, and the Swedish Board for Technical Development. We acknowledge stimulating discussions with J. M. André, A. J. Epstein, A. J. Heeger, and E. J. Mele.

References

1. S. Ikehata, J. Kaufer, T. Woerner, A. Pron, M. A. Druy, A. Sivak, A. J. Heeger and A. G. MacDiarmid, *Phys. Rev. Lett.*, **45**, 1123 (1980).
2. F. Moraes, D. Davidov, M. Kobayashi, T. C. Chung, J. Chen, A. J. Heeger and F. Wudl, *Synth. Met.*, **10**, 169 (1985).
3. K. Kume, K. Mizuno, K. Mizoguchi, K. Nomura, Y. Naniwa, J. Tanaka, M. Tanaka and H. Watanabe, *Mol. Cryst. Liq. Cryst.*, **83**, 285 (1982); F. Maurice, C. Fontaine, A. Morisson, J. Y. Goblet and G. Froyer, *Mol. Cryst. Liq. Cryst.*, **118**, 319 (1985).
4. K. Mizoguchi, K. Misuo, K. Kume, K. Kaneto, T. Shiraishi and K. Koshino, *Synth. Met.*, **18**, 195 (1987).
5. J. M. Ginder, A. F. Richter, A. G. MacDiarmid and A. J. Epstein, *Solid State Commun.*, **63**, 97 (1987); A. G. MacDiarmid, J. C. Chiang, A. F. Richter and A. J. Epstein, *Synth. Met.*, **17**, 285 (1987).
6. X. Q. Yang, D. B. Tanner, M. J. Rice, H. W. Gibson, A. Feldblum and A. J. Epstein, *Solid State Commun.*, **61**, 335 (1987).
7. S. Hasegawa, K. Kamiya, J. Tanaka and M. Tanaka, *Synth. Met.*, **18**, 225 (1987)
8. S. Stafström, J. L. Brédas, A. J. Epstein, H. S. Woo, D. B. Tanner, W. S. Huang and A. G. MacDiarmid, *Phys. Rev. Lett.*, **50**, 1464 (1987).
9. K. Kaneto, S. Hayashi, S. Ura and K. Yoshino, *J. Phys. Soc. Jpn.*, **54**, 1146 (1985).

10. Y. W. Park, Y. S. Lee, C. Park, L. W. Shacklette and R. H. Baughman, *Solid State Commun.*, **63**, 1063 (1987).
11. J. L. Brédas, R. R. Chance and R. Silbey, *Phys. Rev. B*, **26**, 5843 (1982).
12. E. J. Mele and M. J. Rice, *Phys. Rev. B*, **23**, 5397 (1981).
13. A. J. Epstein, in "Handbook of Conducting Polymers," ed. by T. A. Skotheim (Marcel Dekker, New York, 1986), p. 1041.
14. S. Kivelson and A. J. Heeger, *Phys. Rev. Lett.*, **55**, 308 (1985).
15. E. Ehrenfreund, Z. Vardeny, O. Brafman, R. Weagley and A. J. Epstein, *Phys. Rev. Lett.*, **57**, 2081 (1986).
16. H. Y. Choi and E. J. Mele, *Phys. Rev. B*, **34**, 8750 (1986).
17. K. Y. Jen and R. L. Elsenbaumer, *Mol. Cryst. Liq. Cryst.*, this volume.
18. J. L. Brédas and G. B. Street, *Acc. Chem. Res.*, **18**, 309 (1985).
19. M. J. Dewar and W. Thiel, *J. Am. Chem. Soc.* **99**, 4889 (1977); **99**, 4907 (1977).
20. D. S. Boudreaux, R. R. Chance, J. L. Brédas and R. Silbey, *Phys. Rev. B*, **28**, 6927 (1983).
21. S. Stafström and J. L. Brédas, to be published.
22. G. Nicolas and Ph. Durand, *J. Chem. Phys.*, **70**, 2020 (1979), **72**, 453 (1980), and J. M. André, L. A. Burke, J. Delhalle, G. Nicolas and Ph. Durand, *Int. J. Quantum Chem. Symp.*, **13**, 283 (1979).
23. J. L. Brédas, R. R. Chance, R. Silbey, G. Nicolas and Ph. Durand, *J. Chem. Phys.*, **75**, 255 (1981).
24. J. L. Brédas, B. Thémans, J. G. Fripiat, J. M. André and R. R. Chance, *Phys. Rev B*, **29**, 6761 (1984).
25. D. S. Boudreaux, R. R. Chance, J. F. Wolf, L. W. Shacklette, J. L. Brédas, B. Thémans, J. M. André and R. Silbey, *J. Chem. Phys.*, **85**, 4584 (1986).
26. J. L. Brédas, in "Handbook of Conducting Polymers," ed. by T. A. Skotheim (Marcel Dekker, New York, 1986), p. 859.
27. S. Jeyadev and E. M. Conwell, *Phys. Rev. B*, **33**, 2530 (1986).
28. T. C. Chung, F. Moraes, J. D. Flood and A. J. Hegger, *Phys. Rev. B*, **29**, 2341 (1984).
29. T. C. Chung, J. H. Kaufman, A. J. Heeger and F. Wudl, *Phys. Rev. B*, **30**, 702 (1984).